Exploring the astrophysical conditions for the creation of the first r-process peak, and the impact of nuclear physics uncertainties

Stylianos Nikas, G. Martínez-Pinedo, M. R. Wu, A. Sieverding, M. P. Reiter

Exploring the astrophysical conditions for the creation of the first r–process peak, and the impact of nuclear physics uncertainties

S. Nikas[1,2], G. Martínez–Pinedo[1,2], M.R. Wu[3,4,5], A. Sieverding[1,2,6], M.P. Reiter[7,8,9]

[1] *Institut für Kernphysik (Theorizentrum), Fachbereich Physik, Technische Universität Darmstadt, Schlossgartenstraße 2, 64289 Darmstadt Germany*
[2] *GSI Helmholtzzentrum für Schwerionenforschung GmbH, Planckstraße 1, 64291 Darmstadt, Germany*
[3] *Institute of Physics, Academia Sinica, Taipei, 11529, Taiwan*
[4] *Institute of Astronomy and Astrophysics, Academia Sinica, Taipei, 10617, Taiwan*
[5] *National Center for Theoretical Sciences, Physics Division, Hsinchu, 30013, Taiwan*
[6] *School of Physics and Astronomy, University of Minnesota, 116 Church Street SE, Minneapolis 55455, USA*
[7] *II. Physikalisches Institut, Justus–Liebig–Universität, 35392 Gießen, Germany*
[8] *TRIUMF, 4004 Westbrook Mall, Vancouver, British Columbia V6T 2A3, Canada*
[9] *School of Physics and Astronomy, University of Edinburgh, Peter Guthrie Tait Road, EH9 3FD Edinburgh, United Kingdom*

───

Abstract   *We present a study of nucleosynthesis for conditions of high Ye outflows from Neutron Star Mergers (BNSs). We investigate the effect of new beta–decay rates measurements and uncertainties in nuclear masses of the newly measured $^{84,85}Ga$ to the r–process nucleosynthesis calculations. The impact of these quantities to the production of the elements of the r–process abundance pattern for A<100 is quantified and presented. This proceedings paper is based on [1].*

Keywords   *r–process, nucleosynthesis*

───

INTRODUCTION

The rapid neutron capture process (r–process) is responsible for the production of about half of the heavy elements observed in the solar abundances. It is characterized by three peaks, each corresponding to the closed neutron shells at N = 50, 82, 126. The peaks are the result of matter accumulating at the neutron closed shells. The drop in binding energy that characterizes the region after the shell closure leads to a bending of the path towards stability, reaching nuclei with longer β– decay half-lives and producing an accumulation of material, compared to nuclei before or beyond the shell closures.

A site of the r–process was unknown until recent observations. The gravitational wave event GW170817 [2,3] which was identified as a Binary Neutron Star merger (BNS) is considered as a site for the r–process nucleosynthesis [4–9]. The detection of gravitational waves from the binary neutron star was followed by the detection of fast fading optical/infrared counterpart (AT2017gfo) [10], consistent with the predictions for a kilonova, associated with r–process nucleosynthesis [11–15], establishing the production of heavy elements in the aftermath of BNS [15–19]. The complicated atomic structure of lanthanides implies high opacity ejecta; therefore, lanthanides emit light in the red wavelengths, thus, the blue color of the emission spectra at early times indicates that part of the ejecta is characterized by relatively high electron fraction (Y_e) (0.25–0.4) and consequently low lanthanide production [20–26].

Assuming that BNSs are partially responsible for the production of first r–process peak elements, we present a study of nucleosynthesis under moderate Y_e (0.35–0.38) and low entropy (S=10

kB/baryon) conditions. The conditions are consistent with the blue part of the kilonova observation (no lanthanides are created) and provide the strongest contribution to the mass region around the A=80 and A=84. Under these conditions, we investigate the effects of Ga isotopes mass uncertainties and the influence of recently published β–delayed neutron probabilities on the final r–process abundance pattern. We note that the range of Y_e is justified because as shown in [1] lower Y_e (<0.35) leads to overproduction of A=90–120 region whereas Y_e above 0.39 leads to underproduction of the first r–process peak elements.

METHODS

We use the Hauser Feshbach statistical code TALYS [27] to calculate neutron capture reaction rates based on the mass values of the recently measured ^{84,85}Ga. To systematically study the impact of ^{84,85}Ga masses, on the formation of A ≈ 84 nuclei we use a Monte–Carlo approach. We assume the "true" mass value is distributed following a normal distribution with 3σ according to the uncertainty, of their extrapolated mass values given in the atomic mass evaluation data (AME_16) [35] (200, 300 KeV respectively). Table 1 summarizes the new mass measurements and AME_16 corresponding values.

Table 1. *Mass measurements of ^{84,85}Ga isotopes reported in [1] in comparison to AME_16 [35]. The symbol # indicates systematics.*

	Mass excess TITAN (keV/c^2)	Mass excess AME_16 (keV/c^2)	Difference (keV/c^2)
^{84}Ga	−44 094 (30)	−44 090 (200)#	4
^{85}Ga	−39 744 (37)	−39 850 (300)#	−106

Nuclear reaction rates not affected by the new Ga masses measurements were taken from JINA REACLIB [29]. Experimental masses from AME_16 were used when available; otherwise, we use the FRDM mass model [30]. We then use each set of the resulting neutron capture rates in *GSINet* [28] to calculate the r–process abundances.

β–decay rates and β–delayed neutron emission branches were taken from experimentally known nuclear properties database (NUBASE16) [31] when available. When experimental values were not available, values from theoretical predictions [32] were used. Here we included recent β–delayed neutron emission (P_{1n}) of ^{82,83,84,85}Ga [33,34] to study the effect β–delayed–neutron emission branches to the final r–process abundance pattern. The new P_{1n} measurements compared to NUBASE16 are summarized in Table 2.

Table 2. *P_{1n} of ^{82,83,84,85}Ga isotopes reported in [33,34], in comparison to NUBASE16 [35]. The symbol # indicates systematics.*

	Reported at [33,34] P_{1n} (%)	NUBASE16 [31] P_{1n} (%)	Difference (%)
^{82}Ga	22 (2)	21.3 (13)	0.7
^{83}Ga	85 (4)	62.8 (25)	22.2
^{84}Ga	53 (20)	40 (7)	13
^{85}Ga	70 (5)	>35 #	35

The thermodynamic evolution of the systems was parametrized assuming homologous expansion following [36]. The initial temperature was set at T = 6 GK, expansion timescale at 7 ms and entropy

at 10 *kB/baryon.* We perform calculations for Y_e = 0.35–0.38. Different electron fraction results were considered with equal weight.

RESULTS

We compare our results with the solar r–process abundances (Fig. 1) in the region A≈80–90. The pink uncertainty bands show the variation of the abundances that arise from the uncertainties of the masses of ^{84,85}Ga from AME_16. The new Ga mass values affect the abundances of elements with mass number A=82–87, with the biggest impact on A=83 accounting to ≈10% despite the small change in mass value. The uncertainty band also shows that under some combinations of ^{84}Ga and ^{85}Ga masses within their corresponding error bars the peak at A=84 is severally under–produced.
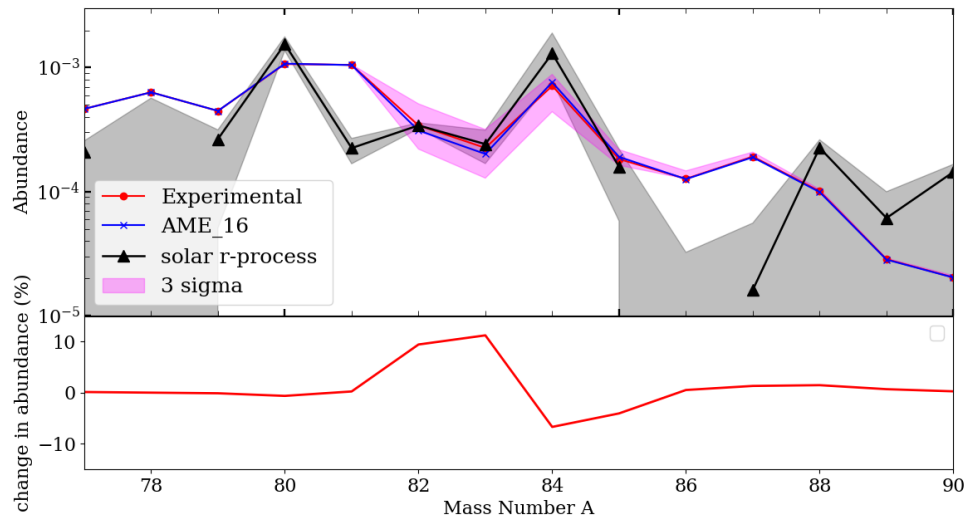

Figure 1. (*Upper plot) Final abundances averaged over calculations with Y_e =0.35–0.38 compared to the solar r–process abundance, with uncertainty shown as a gray band. The pink band shows the 3σ change in calculated production, a result of the variation of the masses of ^{84,85}Ga. The red line shows the resulted abundances using the central experimental value whereas the blue line the abundances when the AME_16 extrapolated mass values were used. (Lower plot) Change, in percentage, of the abundance pattern as a result of using the mass values from [1] compared to the extrapolations given in the AME_16. Figure adapted from [1]*

Similarly, in Fig. 2 we compare our results with the solar r–process for two separate cases; in the first case, we use data for β–delayed neutron emission branches from NUBASE16. In the second case, we use the updated data for ^{82,83,84,85}Ga as presented in Table 2 from [33,34]. The differences are more pronounced at A=85 where the 2 instances of our calculations differ by ~18%. This difference can be traced back to the changed by ~35 % value of P_{1n}, where NUBASE16 value was given as ~35%, and [34] measurement at ~70 (5) %.

CONCLUSIONS

We explored the impact of a series of newly measured Ga isotopes. We demonstrate that at moderate neutron–rich conditions, realized in BNSs, r–process calculations can produce the local peaks at A = 80 and A = 84 of the solar system r–process residual. We show that changes of only a few keV in the mass of a single nucleus can lead to differences in abundances of more than 10%. In addition, we demonstrate the impact of β–delayed neutron emissions, finding changes of ~18% in

abundances of A=85 calculations using the NUBASE16 data, compared to NUBASE16 updated with the ^{82,83,84,85}Ga P_{1n} values according to [33,34].
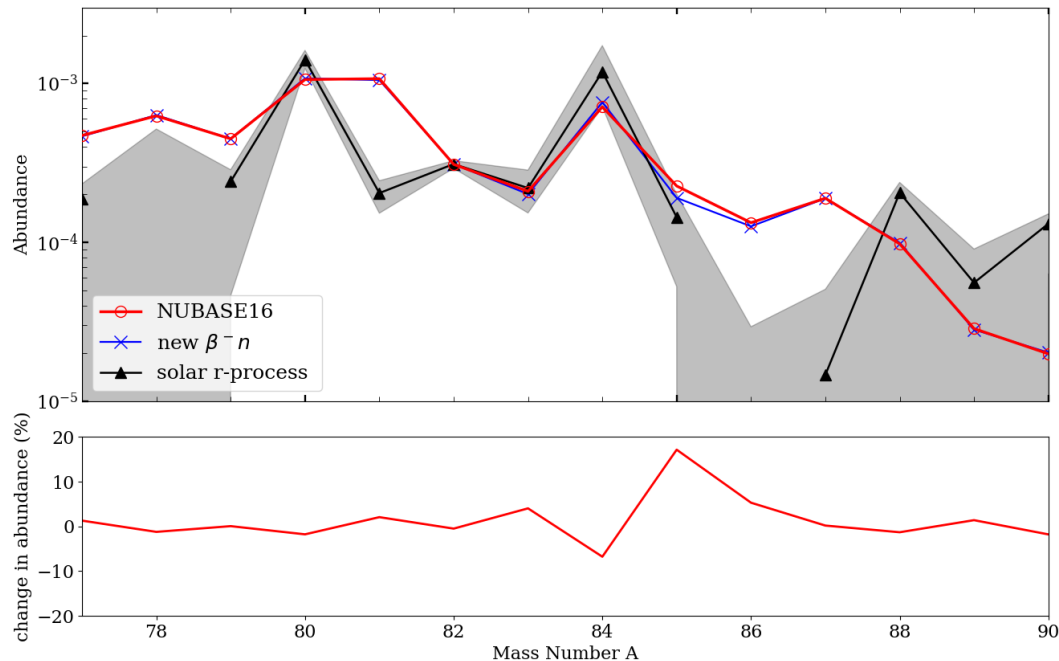

Figure 2. (*Upper plot) Final abundances averaged over calculations with Ye = 0.35–0.38 compared to the solar r–process abundance, with uncertainty shown as gray band. The red line corresponds to abundances when NUBASE16 was used for β–delayed neutron emission probabilities, while the blue line corresponds to abundances when the measured [33,34] β–delayed neutron emission probabilities of Ga 82–85 were used to update NUBASE16 values. (Lower plot) Change, in percentage, of the abundance pattern as a result of using the β–decay ratios and β–delayed neutron emission probabilities values from [33,34] compared to the values given in NUBASE16.*

Acknowledgments

References

[1]   M.–P. Reiter et al., Phys. Rev. C, 101 025803. (2020).
[2]   B.P. Abbott et al., Phys. Rev. Lett. 119, 161101 (2017).
[3]   B. P. Abbott et al., Astrophys. J. Lett. 848, L13 (2017)
[4]   J. M. Lattimer and D. N. Schramm, Astrophys. J. 192, L145 (1974).
[5]   J. M. Lattimer and D. N. Schramm, Astrophys. J. 210, 549 (1976).
[6]   D. Eichler et al., Nature 340, 126 (1989).
[7]   S. Rosswog et al., Astron. Astrophys. 341, 499 (1999).
[8]   C. Freiburghaus, S. Rosswog, and F.–K. Thielemann, Astrophys. J. Lett. 525, L121 (1999).
[9]   M. Arnould, S. Goriely, and K. Takahashi, Phys. Rep. 450, 97 (2007).
[10] B. P. Abbott et al., Astrophys. J. Lett. 848, L12 (2017).

[11] L.–X. Li and B. Paczyński, Astrophys. J. 507, L59 (1998).
[12] B. Metzger et al., Mon. Not. R. Astron. Soc. 406, 2650 (2010).
[13] L. F. Roberts et al., Astrophys. J. 736, L21 (2011).
[14] A. Bauswein, S. Goriely, and H.–T. Janka, Astrophys. J. 773, 78 (2013).
[15] R. Fernández and B. D. Metzger, Annu. Rev. Nucl. Part. Sci. 66, 23 (2016).
[16] B.P. Abbott et al., Astrophys. J. Lett. 848, L12 (2017).
[17] N.R. Tanvir et al., Astrophys. J. 848, L27 (2017).
[18] R. Chornock et al., Astrophys. J. 848, L19 (2017).
[19] E. Pian et al., Nature 551, 67 (2017).
[20] P. Evans et al., Science 358, 1565 (2017).
[21] S.J. Smartt et al., Nature 551, 75 (2017).
[22] E. Troja et al., Nat. Commun. 9, 4089 (2018).
[23] M. Nicholl et al., Astrophys. J. 848, L18 (2017).
[24] S. Rosswog et al., Astron. Astrophys. 615, A132 (2018).
[25] S. Wanajo, Astrophys. J. 868, 65 (2018).
[26] M.–R. Wu et al., Phys. Rev. Lett. 122, 062701 (2019).
[27] A. J. Koning, S. Hilaire, and M. C. Duijvestijn, in Proceedings of the International Conference on Nuclear Data for Science and Technology (EDP Sciences, Paris, France, 2007), pp. 211–214.
[28] J. J. Mendoza–Temis et al., Phys. Rev. C 92, 055805 (2015).
[29] R.H. Cyburt et al., Astrophys. J., Suppl. Ser. 189, 240 (2010).
[30] P. Moeller et al., At. Data Nucl. Data Tables 109–110, 1 (2016).
[31] G. Audi et al., Chin. Phys. C 41, 030001 (2017).
[32] P. Möller, B. Pfeiffer, and K.–L. Kratz, Phys. Rev. C 67, 055802 (2003).
[33] D. Verney et al., Phys. Rev. C 95, 054320 (2017).
[34] K. Miernik et al., Phys. Rev. C 97, 054317 (2018).
[35] M. Wang et al., Chin. Phys. C 41, 030003 (2017).
[36] J. Lippuner and L. F. Roberts, Astrophys. J. 815, 82 (2015).